1994A&A...287..552O

Astron. Astrophys. 287, 552–558 (1994)

ASTRONOMY AND ASTROPHYSICS

The OH/IR-planetary nebula connection: space distribution and kinematics

R. Ortiz and W.J. Maciel

Instituto Astronômico e Geofísico da USP, Av. Miguel Stefano 4200, CEP 04301-904 São Paulo SP, Brazil

Received 20 September 1993 / Accepted 25 February 1994

Abstract. We investigate the connection between AGB stars, especially OH/IR stars, and planetary nebulae (PN). The latter comprise a mixed population, with a range of spatial and kinematical properties, attributed to the age and mass of the progenitor star. We propose a classification scheme for OH/IR stars based on the separation of the OH peaks and the IRAS [12-25] colour index. It is shown that the OH/IR stars can be separated into classes with spatial and kinematical characteristics resembling those of the corresponding PN types.

Key words: stars: AGB, post-AGB – stars: fundamental parameters – planetary nebulae: general – Galaxy: stellar content

1. Introduction

OH/IR stars are giants of intermediate masses, which are losing mass at a high rate ($10^{-7} \sim 10^{-4} M_{\odot}$ year^{-1}) in the AGB phase. They can be detected by infrared surveys (e.g. Two micron sky survey, IRAS) and/or by radio surveys in the 18 cm OH transition lines (1612, 1665, 1667, and 1670 MHz). It is generally believed that they form the last stage of stellar evolution before the ejection of the hydrogen envelope and the formation of a planetary nebula (Habing et al. 1989). However, the transition between the AGB and the PN phases occurs very rapidly (less than 10^4 years), and is still poorly known. On the other hand, both kinds of objects must have similar properties, such as the space distribution and kinematics.

Since the discovery of the OH/IR phenomenon by Wilson & Barret (1968), several attempts for the classification of these objects were made. Baud et al. (1981, hereafter BHMW), and more recently te Lintel Hekkert (1990), divided the objects into two classes, according to the separation of their OH peaks. In particular, their results indicate that objects with higher expansion velocities ($\Delta V > 29$ km/s) have radial velocities which can be associated with the rotation curve of the Galaxy, and are identified as supergiants, while the low velocity group was associated with Mira variables.

Send offprint requests to: R. Ortiz

The space distribution and kinematics of PN have been recently studied by Maciel & Dutra (1992, hereafter MD). In the framework of the classification system originally proposed by Peimbert (1978), it was shown that there is a closer association of PN types I and II with the motion of disk stars, as measured by the galactic rotation curve. Also, the analysis of chemical abundances and radial gradients (Maciel & Köppen 1993) indicate that type I nebulae have strong He/H and N/O enhancements, which are interpreted as evidences of higher progenitor masses and relatively younger ages.

In this paper we investigate further the connection between OH/IR stars and planetary nebulae, and propose a classification scheme of OH/IR stars based on their expansion velocities as well as their IRAS colours.

2. The database

OH/IR stars are usually discovered by means of radio surveys of the 18 cm OH maser emisssion towards infrared sources with colour indexes inside a colour window obtained from well-known objects. Sometimes, the inverse procedure is applied, and the infrared counterpart of a known OH source is obtained. Type II OH masers, detected mainly at 1612 MHz, are believed to be of stellar origin.

Our sample consists of about 1500 objects extracted from the literature, comprising radio and infrared data. te Lintel Hekkert et al. (1989) compiled 442 1612 MHz sources published up to 1983. Since then, systematic surveys have been conducted by several groups, such as the Arecibo, Nançay, and the Parkes teams (cf. Eder et al. 1988; Likkel 1989; te Lintel Hekkert et al. 1991; Sivagnanam et al. 1990). The main results of these groups are summarized in Table 1. A complete and updated catalogue on these sources is under preparation. The catalogue used in this work consists of: (1) IRAS name; (2) [12], [25] and [60] IRAS magnitudes; (3) galactic coordinates; (4) radial velocities of the peaks; (5) J, H, K, L, and M magnitudes (when available); (6) name of the counterpart(s).

The PN data used as a comparison has been discussed by Maciel & Dutra (1992), supplemented by the chemical compositions given by Maciel & Köppen (1993) and Chiappini &

© European Southern Observatory • Provided by the NASA Astrophysics Data System

1994A&A...287..5520

Table 1. The OH/IR database

Reference	Number of objects	Frequency (MHz)
David et al. (1993a)	131	1667
David et al. (1993b)	41	1612
Dickinson & Turner (1991)	41	1665,1667
Eder et al. (1988)	184	1612
Galt et al. (1989)	25	1612
Le Squeren et al. (1992)	74	1612,1667
Lewis et al. (1985)	21	1612
Lewis et al. (1990)	86	1612
Likkel (1989)	21	1612,1667
Sivagnanam et al. (1988)	14	1612,1665,1667
Sivagnanam et al. (1990)	36	1612,1667
te Lintel Hekkert et al. (1989)	442	1612
te Lintel Hekkert et al. (1991)	738	1612

Maciel (1993). About 200 disk objects are included, for which distances, radial velocities and abundances are known.

3. Space distribution of OH/IR stars

3.1. Latitude distribution

Systematic surveys conducted during the last few years allow us to study the space distribution of OH/IR stars in the Galaxy, in particular in the direction perpendicular to the galactic plane. BHMW and te Lintel Hekkert & Zijlstra (1991) showed that low-expansion velocity objects have a vertical distribution that resembles that of PN, while high expansion velocity objects have been associated with supergiant stars and show a vertical distribution distinct from that of planetary nebulae. However, no account has been taken of the variety of types that make up the system of planetary nebulae. In fact, MD have shown that Peimbert's types I to IV form an approximately continuous sequence in terms of average heights from the galactic plane. This sequence is actually a sequence of mass of the progenitor star, which increases towards the earlier types. A comparison between OH/IR stars and planetary nebulae must consider that both groups comprise mixed populations with distinct characteristics such as ages, masses and chemical composition (cf. Maciel & Köppen 1993).

Figure 1 shows histograms of the galactic latitude for (a) high ($\Delta V > 35$ km/s) and (b) low ($\Delta V < 20$ km/s) expansion velocities of the OH shell. The definition of these limits will be commented upon later in this paper. It can be seen that the objects with higher velocities are in average closer to the galactic plane, so that they are probably more massive and younger than the low velocity objects.

The dependence of the circumstellar envelope expansion velocity with the physical parameters of the central star and of the envelope itself is still poorly known. The OH maser emission is pumped by 35 μm infrared photons. The stellar radiation field interacts with the material in the envelope, being absorbed and scattered selectively. Thus, a fraction of the 35 μm photons originates in the envelope, which is moving outwards from the star, accelerated by the radiation pressure on grains. The momentum that pushes the grains, and consequently their final drift velocity, depends on the luminosity of the central star. This can be calculated by the empirical "Paczinski relation", which gives L_{star} as a function of the core mass, which is roughly proportional to the stellar mass. The expansion velocity of the envelope depends also on the metallicity, since the formation of grains implies some depletion of metallic molecules such as SiC or SiO.

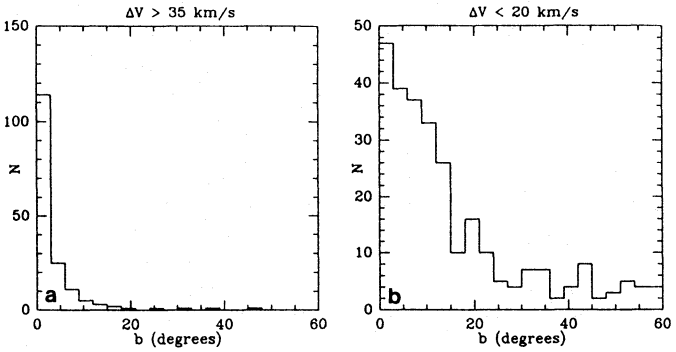

Fig. 1a and b. Galactic latitude distribution of **a** high and **b** low expansion velocity OH/IR stars

3.2. Distances to OH/IR stars

The results shown in Fig. 1 can be given some support by taking into account the height distribution of the OH/IR stars, provided we are able to make reliable estimates of their distances.

First, we have determined kinematical distances for stars with double-peaked OH emission. Since the double-peak feature is caused by the Doppler effect due to the expansion of the circumstellar OH envelope, the mean peak velocity is a good approximation for the stellar velocity. We assume the rotation curve for the Galaxy given by Clemens (1985), with $R_0 = 8.5$ kpc. The fraction of objects with no kinematical solution is small (cf. Fig. 4). For objects in the first and fourth quadrants, where the distance problem cannot be resolved univocally, we adopt the shortest kinematical distance. Although this hypothesis may not be always correct, the kinematical distances (and heights) can be statistically considered as lower limits.

Second, we developed an alternative method for the calculation of distances that we call "infrared distance". Feast et al. (1989) determined a period-luminosity (PL) relationship for oxygen-rich Miras in the LMC. The average bolometric magnitude is described as a linear function of the period of the star. Although we do not know the period, except for a few well-studied objects, it can be inferred from a period-ΔV relationship derived by Dickinson et al. (1975). We improved their sample with data from Engels et al. (1981), totalizing 47 objects with well-determined periods. The following formula was used:

© European Southern Observatory • Provided by the NASA Astrophysics Data System

1994A&A...287..5520

$$< M_{\rm bol} >= 2.88 - 3.00 \log(222 + 17.4\Delta V) \quad (1)$$

where ΔV is in km/s. We integrated the infrared energy distribution of OH/IR stars of our sample for which near-infrared photometry was available. The infrared magnitudes were converted into flux densities using the zero-magnitude fluxes given by Koorneeff (1983) and then corrected for interstellar extinction, based on a model for the Galaxy by Ortiz & Lépine (1993). The integration ends at $\lambda = 60\mu m$. The flux contribution beyond this limit may be estimated by the use of a bolometric correction. We assume a power-law spectrum $f(\nu) \sim \nu^{\alpha}$ between $\lambda = 60\mu m$ and $\lambda = 100\mu m$. It can be shown that:

$$\alpha = \frac{{\rm d}\log f_\nu}{{\rm d}\log \nu} = -4.51 \log\left(\frac{f_{100}}{f_{60}}\right) \quad (2)$$

Gaylard & Whitelock (1988) studied an IRAS based sample of OH/IR stars with good quality flux densities f_{60} and f_{100}. From Table 3 of their paper we have $< \log f_{100}/f_{60} >= -0.51$ which, if applied to Eq. (2) yields $\alpha = 2.31$. Thus OH/IR stars can be approximated, near $\lambda = 100\mu m$, by a Rayleigh-Jeans spectrum. Integrating f in frequency between $\nu = 0$ and $\nu = c/60\mu m$, where c is the speed of light, we get:

$$I = \frac{\nu_{60} f_{60}}{1+\alpha} \quad (3)$$

where I represents the apparent flux of the star beyond $\lambda = 60\mu m$ to be added to the flux integral.

In order to test the validity of this method, we compared the *infrared* distances with *geometric* distances given by Herman et al. (1986) and van Langevelde et al. (1990). The latter is a very precise method, which compares the angular size of the OH envelope (measured by VLA) and the phase lag of the two OH peaks. The authors estimate a precision for the distance better than 20%. The comparison between $d_{\rm IR}$ and $d_{\rm geo}$ showed a fair correlation, with some scatter due mainly to the variability of $M_{\rm bol}$ and the scattering of the period-ΔV relationship.

On the other hand, a comparison of our *kinematical* distances with the *infrared* distances shows that $d_{\rm kin} >> d_{\rm IR}$ for $\Delta V < 20$ km/s, and $d_{\rm kin} \sim d_{\rm IR}$ for $\Delta V > 35$ km/s, except for a few stars at very large (> 10 kpc) kinematical distances. This suggests that the objects with higher expansion velocities have approximately correct distances, and are consistently more closely associated with the rotation of the galactic disk. Histograms of the *distance* to the galactic plane instead of the galactic *latitude* show therefore essentially the same behaviour displayed in Fig. 1. A discussion of the absolute scale heights for OH/IR stars in comparison with galactic planetary nebulae will be made in Sect. 4.

3.3. Infrared colours and mass loss

Another piece of evidence on the space distribution of OH/IR stars comes from Fig. 2, where we show histograms of the galactic latitude for three ranges of the infrared colour index [12]-[25], namely: (a) [12]-[25]>2.5, (b) 1.5<[12]-[25]<2.5, and (c) [12]-[25]<1.5. It can be seen from the histograms that the reddest OH/IR stars are, in average, closer to the galactic plane, when compared with bluer objects. The effect of interstellar reddening can be discarded at these wavelenghts, even if the objects are far away in the galactic plane. In fact, the same behaviour can be observed taking another infrared colour index, such as I-K, J-K, K-L, etc. This is an indication that the ΔV criterion is not sufficient to explain the latitude distribution of OH/IR stars, i.e. there seems to exist a group of stars with large colour indices and low distances to the galactic plane, irrespective of the velocity separation of their OH peaks (see Sect. 4). In fact, the ΔV criterion does not work well alone, due to its strong dependence on the metallicity. The depletion of metals onto grains improve the efficiency of the acceleration mechanism of the circumstellar material, increasing its expansion velocity. Blommaert (1992) studied a sample of OH/IR stars near the galactic centre. He concluded that there seems to exist two groups of stars, divided on the basis of their expansion velocities. The high V_{exp} group is believed to be more metal-rich than the low expansion velocity group. On the other hand, Wood et al. (1992) discovered 6 OH/IR stars in the LMC. They observed that their expansion velocities are about 0.6 times those expected for similar OH/IR stars in our Galaxy, and interpreted the discrepancy as being due to the lower metal abundance in that galaxy ([Fe/H] = -0.3 dex, Russel & Bessell 1989).

OH/IR stars have optically-thick dust envelopes, accelerated by radiation pressure on grains. Assuming a perfect coupling between dust and gas, and gravitational effects negligible when compared with the radiative force, Salpeter (1974) derived the relationship:

$$\dot{M} V_{\rm e} \sim \frac{\tau_{\rm dust} L_{star}}{c} \quad (4)$$

where $\dot{M}$ is the mass loss rate, $V_{\rm e}$ is the expansion velocity of the envelope, L_{star} the luminosity of the star, c the speed of the light and $\tau_{\rm dust}$ the optical depth of the dust. Unfortunately, $\tau_{\rm dust}$ must be inferred by dust shell modelling, which depends on detailed observations in a large range of wavelengths. On the other hand, Bedijn (1987) suggested a linear relationship involving $\tau_{\rm dust}$ and the f_{25}/f_{12} ratio. van der Veen & Rugers (1989) studied a sample of about 60 O-rich stars in order to obtain a calibrated relationship for the mass loss of OH/IR stars. They found that:

$$\dot{M} = 1.3 \times 10^{-5} \frac{L_4}{V_{15}} \left(\frac{f_{25}}{f_{12}}\right)^{2.9} M_\odot/{\rm year} \quad (5)$$

where L_4 is the luminosity of the star in units of $10^4 L_\odot$ and V_{15} the expansion velocity of the envelope in units of 15 km/s.

© European Southern Observatory • Provided by the NASA Astrophysics Data System

1994A&A...287..5520

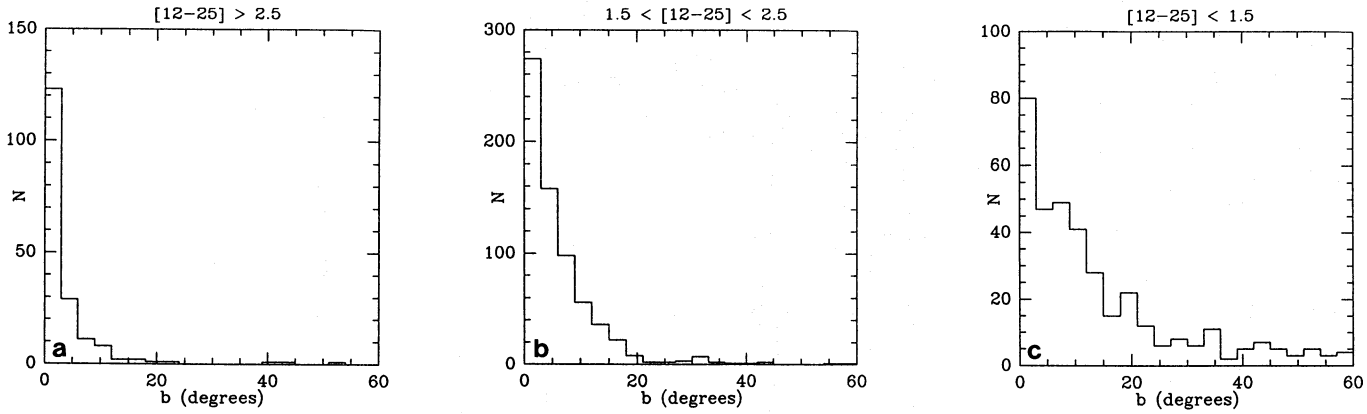

Fig. 2a–c. Galactic latitude distribution for OH/IR stars, according to the [12-25] color index

Assuming an average bolometric magnitude $< M_{\rm bol} >= -6.6$ (Gaylard & Whitelock 1988), and a typical expansion velocity $V_{\rm e}$ = 15 km/s, the mass loss may be estimated for several colour ranges, such as those in Fig. 2. For the reddest objects ([12 − 25] > 2.5), which are closer to the galactic plane, mass loss can exceed $\dot{M} \gtrsim 5 \times 10^{-4} M_{\odot}$ /year, while for the bluer ones ([12 − 25] < 1.5) $\dot{M} \lesssim 4 \times 10^{-5} M_{\odot}$/year.

We have seen that the vertical distribution of the reddest objects indicates that they must be younger than bluer objects. From Eq. (5) their f_{25}/f_{12} ratio suggests they are losing mass at a higher rate. Both phenomena can be interpreted as an indication that the mass of an OH/IR star increases, in average, with its colour index.

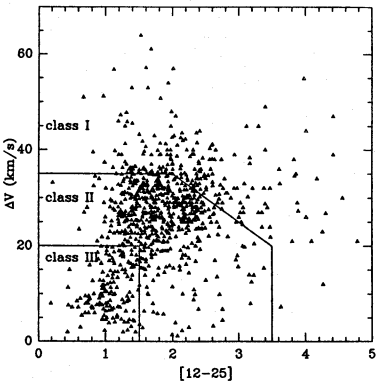

Fig. 3. Classification of OH/IR stars according to the velocity separation of the OH peaks and the [12-25] color index

4. Classification of OH/IR stars

In view of the results of Sect. 3, it seems reasonable to propose a classification scheme of OH/IR stars which take into account both the space distribution and colours of these objects. As mentioned in the introduction, OH/IR stars do not represent a single class of objects and BHMW have already divided them into two groups, according to their expansion velocity. Therefore, we have assembled the information of Figs. 1 and 2 on the vertical distribution and infrared colours, and divided the [12-25] × ΔV plane into 3 regions, where we can identify stars of classes I, II and III (Fig. 3). We have calculated for each region the mean and the median scale height of the objects from their kinematical distances, as given in Table 2. Qualitatively similar results can be obtained from infrared distances.

It can be seen that the objects of class I have larger velocity separations and/or redder colours, and are associated with the younger populations closer to the galactic plane, in the same sense as the type I planetary nebulae. Class II OH/IR stars occupy an intermediate position on the ΔV × [12]-[25] plane, and class III show the largest scale heights, which can be associated with type III PN. Therefore, by comparing the OH/IR stars scale heights with the results by MD, also given in Table 2, we are able to establish a one-to-one correspondence between OH/IR stars and planetary nebulae. As we will see in the next section, kinematic data strongly support this classification.

Assuming an exponential vertical distribution of stars, $N \sim \exp -(|z|/H)$, the derived scale height H, which is equivalent to $< |z| >$, is in good agreement with the values given in Table 2. Knowledge of scale heights allow us to obtain typical masses of the progenitor stars. We have used the compilation by Rana (1987), based on data on scale heights and ages collected from the literature.

According to his data, class I OH/IR stars (and type I PN) have progenitor masses greater than 1.4 $M_{\odot}$ and ages less than 2 Gyr. This result is not exactly the same found by BHMW, who associated high ΔV OH/IR stars with M supergiants. In fact, those objects are included in our class I, but relatively young supergiant stars comprise the minority of high ΔV objects.

Class II comprises ZAMS masses between 1.0 and 1.4 $M_{\odot}$ and ages between $2 \times 10^9 \sim 9 \times 10^9$ years, somewhat younger than the disk of the Galaxy which is thought to be between 9 and 15 Gyr (Miller & Scalo 1979). Class III OH/IR stars have masses less than $1.0 M_{\odot}$ and are older than 9 Gyr.

These characteristics are consistent with the evolution of OH/IR stars towards PN, and the estimated ages are in agreement with PN ages derived by Maciel & Köppen (1993) and Freitas Pacheco (1993), on the basis of age-metallicity relationships.

© European Southern Observatory • Provided by the NASA Astrophysics Data System

1994A&A...287..5520

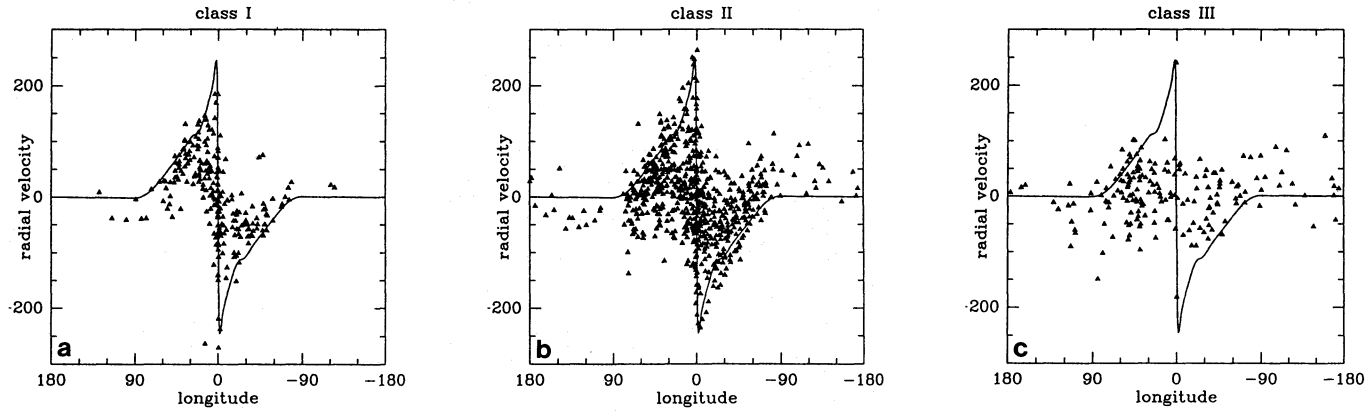

Fig. 4a–c. Galactic longitude distribution of radial velocities for OH/IR stars according to their classification: **a** I, **b** II and —bf c III. The continuous line shows the velocities implied by the Clemens (1985) rotation curve

Where are class IV OH/IR stars? In our sample, we could not find objects whose characteristics resemble those of type IV planetary nebulae. Such stars would be so old and metal-poor that the oxygen abundance in the envelope would probably not supply the necessary amount of molecules such as OH or TiO. Thus, OH maser phenomenon would not be observed for these stars, and their spectra should contain rotational molecular features (such as TiO or ZrO bands) indicating very low metallicities. A search for metal-poor, AGB stars with halo kinematics could, in principle, identify the precursors of type IV planetary nebulae.

From Fig. 3 it becomes clear that the IRAS colour criterium is necessary to have a better understanding of the OH/IR stars. It can be seen that a reasonably large group of stars have low ($\Delta V < 30$ km/s) velocities and still maintain the characteristics of class I, being precisely those with redder ($[12-25] > 3$) colours. As an example, if we select a subsample of stars defined by the criteria $\Delta V < 30$ km/s and $[12-25] > 3$ we obtain the following results: $< |Z| >= 190$ parsecs and $|Z|_{1/2} = 60$ parsecs, indicating that these red, low expansion velocity stars are concentrated near the galactic plane, which is a characteristic of young objects (see Table 2).

Our proposed classification scheme for OH/IR stars shows some differences relative to earlier attempts (e.g. BHMW, te Lintel Hekkert et al. 1991; te Lintel Hekkert & Zijlstra 1991), especially regarding the comparison with planetary nebulae. This can be partially attributed to our detailed consideration of the subgroups that comprise the PN population, as made clear by MD and Maciel & Köppen 1993. However, it should be stressed that our results on the classification of OH/IR stars confirms the previous work in the sense that *younger* populations of these stars are identified with objects with *higher* expansion velocities.

5. Kinematics

5.1. Longitude distribution and peculiar velocities

Having established that the separation ΔV of the OH peaks is correlated with the space distribution and infrared colours of OH/IR stars, it is interesting to investigate whether similar correlations exist regarding the kinematical properties of these objects, which are essentially measured by the radial velocities and the expected velocities consistent with the galactic rotation curve.

Table 2. Average heights from the galactic plane and peculiar velocities

Type	N	$< \|Z\| >$ (parsec)	$\|Z\|_{1/2}$ (parsec)	N	$< \|\delta V\| >$ (km/s)	$\|\delta V\|_{1/2}$ (km/s)
PN-I	53	150	110	38	20.5	17.2
PN-II	60	350	240	57	21.7	20.9
PN-III	33	660	410	29	64.0	57.1
PN-IV	6	7200	6900	4	172.8	167.2
OH/IR-I	209	150	50	22	18.0	17.5
OH/IR-II	571	370	190	85	27.9	21.0
OH/IR-III	106	760	500	34	32.2	26.1

BHMW showed that high expansion velocity OH/IR stars follow the rotation curve of the Galaxy more closely, and associated them with M supergiants with ages less than 10^7 years. Our results indicate that the high expansion velocity OH/IR stars and also the reddest ones (our class I objects) have smaller random motions with respect to galactic rotation.

This can be seen in Fig. 4 which is a plot of the radial velocities against longitude for OH/IR stars of classes I, II and III, respectively. The solid line represents the boundaries defined by the galactic rotation curve as given by Clemens (1985). The general similarity of the longitude distribution of OH/IR stars with that of planetary nebulae (cf. Maciel 1989) is clear, as has been pointed out before (cf. Habing et al. 1989; Pottasch 1984). It can be further concluded that our class I objects follow more closely the rotation curve when compared with older, less massive, class III OH/IR stars.

For a star with galactic coordinates (l, b), the deviations from the galactic rotation curve can also be quantified by the peculiar radial velocity δV, defined as:

© European Southern Observatory • Provided by the NASA Astrophysics Data System

1994A&A...287..5520

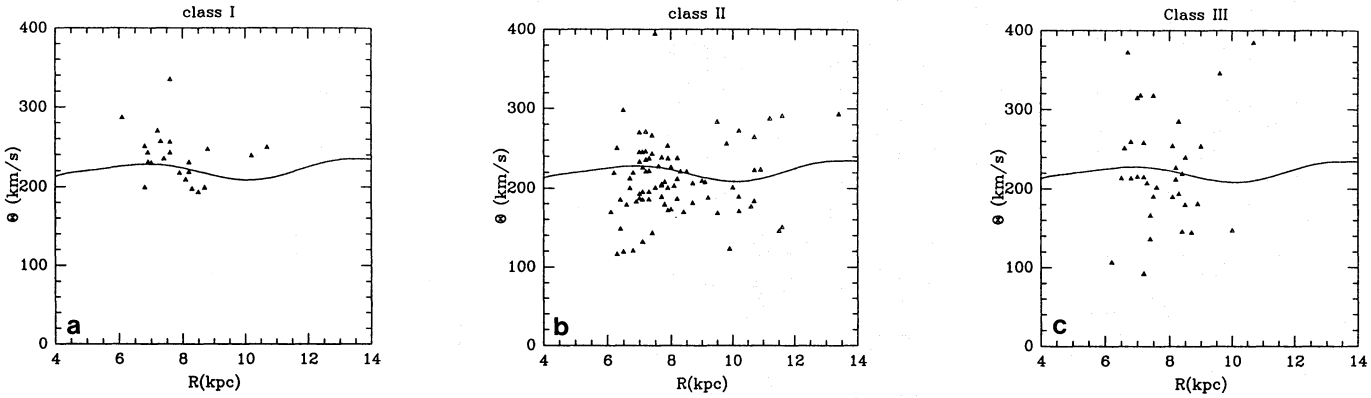

Fig. 5a–c. Rotation velocities as a function of the galactocentric distance R, for OH/IR stars (triangles) for **a** class I, **b** II, and **d** III. The continuous line shows the rotation curve by Clemens (1985)

$$\delta V = V_{\rm LSR} - R_0 \left(\frac{\Theta(R)}{R} - \frac{\Theta_0}{R_0} \right) \sin l \cos b \qquad (6)$$

where $\Theta(R)$ is the rotation velocity at the galactocentric distance R, which is calculated from the infrared distance mentioned in Sect. 3, and $V_{\rm LSR}$ is the radial velocity with respect to the Local Standard of Rest.

A comparison between our results and those found by MD is also given in Table 2. It can be seen that the mean and median values of δV increase from earlier to later types of both PN and OH/IR stars. The δV values of planetary nebulae are in good agreement with those of their precursors, except for class III objects. We believe this discrepancy is not serious because this class of objects can reach great distances from the galactic plane, where circular orbits are not an adequate hypothesis.

Wielen (1977) showed that the increase with age of the stellar velocity dispersion may be caused by the existence of an irregular gravitational field such as that originated by giant molecular clouds. From the time dependence of the velocity dispersion and the average peculiar velocities of Table 2, we obtained for class I OH/IR stars an age of about 1.5 Gyr, compatible with our previous result based on the scale height. The vertical dispersion was estimated to be about 130 parsecs, similar to the value we found in Table 2. The stellar velocity dispersion of class II OH/IR stars suggests an age about 4.5 Gyr and a vertical dispersion of 190 parsecs. We did not compare Wielen's results with ours for class III OH/IR stars, since high latitude kinematical data are unreliable in this case.

5.2. OH/IR stars and the PN rotation curve

In the work of Maciel & Dutra (1992) it was shown that planetary nebulae of the earlier types (I/IIa) can be used in order to determine the galactic rotation curve, as their peculiar velocities are only marginally larger than those of extreme population I objects such as the galactic HII regions. In order to investigate further the connection of OH/IR star and planetary nebulae, we have compared the rotation velocities $\Theta(R)$ of the former with the galactic rotation curve, as was done by MD for the planetary nebulae. We adopted our infrared distances in order to obtain the linear velocities $\Theta(R)$ plotted in Fig. 5. We excluded from the study objects with galactocentric distances less than 6 kpc, so that we have approximately the same distance range studied by MD. The solid line in Fig. 5 shows the rotation curve given by Clemens (1985), and should be compared with Fig. 4 of MD. It can be seen that the scattering increases from earlier to later classes OH/IR stars, indicating that younger, more massive class I stars are kinematically closer to the rotation curve when compared with older, less massive class III objects. Although infrared distances are uncertain, the smooth behaviour of the rotation curve near R_0 indicates that the comparison is consistent. Therefore, the rotation curve supports our classification scheme of OH/IR stars in three classes, in good agreement with the Peimbert PN types. An immediate consequence is that class I OH/IR stars could in principle be used to derive the rotation curve of the outer Galaxy, where the uncertainty in the determination of this curve is higher (see for example Brand & Blitz 1993). The 18 cm OH transitions can be measured very precisely in these objects, which implies a good determination of the radial velocities. On the other hand, OH/IR stars become rarer at $R > R_0$, where carbon stars take their place and the ratio O/C < 1 due to the radial oxygen abundance gradient (Maciel & Köppen 1993).

Acknowledgements. We thank Jacques R.D. Lépine and Pascal Fouqué for their participation in the catalogue making. This work was supported by FAPESP under grant 91/2315-8 and by CNPq.

References

Baud, B., Habing, H.J., Matthews, H.E., Winnberg. A., 1981, A&A 95, 156 (BHMW)
Bedijn, P.J., 1987, A&A 186, 136
Blommaert, J., 1992, PhD Thesis, Leiden
Brand, J., Blitz, L. 1993, A&A 275, 67
Chiappini, C.M.L., Maciel, W.J., 1993, A&A (submitted)
Clemens, D.P., 1985, A&A 295, 422
David, P., Le Squeren, A.M., Sivagnanam, P., Braz, M.A., 1993a, A&AS 98, 245
David, P., Le Squeren, A.M., Sivagnanam, P., 1993b, A&A, 277, 453

© European Southern Observatory • Provided by the NASA Astrophysics Data System

1994A&A...287..5520

Dickinson, D.F., Turner, B.E., 1991, ApJS 75, 1323
Dickinson, D.F., Kollberg, E., Yngvesson, S., 1975, ApJ 199, 131
Eder, J., Lewis, B.M., Terzian, Y., 1988, ApJS 66, 183
Engels, D., Schultz, G.V., Sherwood, W.A., 1981, in Physical processes in red giants, eds. I. Iben Jr., A. Renzini, p.401
Feast, M.W., Glass, I.S., Whitelock, P.A., Catchpole, R.M., 1989, MNRAS 241, 375
Freitas Pacheco, J.A., 1993, ApJ 403, 673
Galt, J.A., Kwok, S., Frankow, J., 1989, AJ 98, 2182
Gaylard, M.J., Whitelock, P.A., 1988, MNRAS 235, 123
Habing, H.J., te Lintel Hekkert, P., van de Veen, W.E.C.J., 1989, IAU Symp. 131, ed. S. Torres-Peimbert, Kluwer, p. 359
Herman, J., Burger, J.H., Penninx, W.H., 1986, A&A 167, 247
Koornneef, J., 1983, A&A 128, 84
Le Squeren, A.M., Sivagnanam, P., Dennefeld, M., David, P., 1992, A&A 254, 133
Lewis, B.M., Eder, J., Terzian, Y., 1985, Nat 313, 200
Lewis, B.M., Eder, J., Terzian, Y., 1990, ApJ 362, 634
Likkel, L., 1989, ApJ 344, 350
Maciel, W.J., 1989, IAU Symp. 131, ed. S. Torres-Peimbert, Kluwer, p. 73
Maciel, W.J., Dutra, C.M., 1992, A&A 262, 271 (MD)
Maciel, W.J., Köppen, J., 1993, A&A (in press)
Miller, G.E., Scalo, J.M., 1979, ApJS 41, 513
Ortiz, R., Lépine, J.R.D., 1993, A&A 279, 90
Peimbert, M., 1978, in IAU Symposium 76, ed. Y.Terzian, Reidel, Dordrecht, p.215
Pottasch, S.R., 1993, Planetary Nebulae, Reidel
Rana, N.C., 1987, A&A 184, 104
Russel, S.C., Bessell, M.S., 1989, ApJS 70, 865
Salpeter, E.E., 1974, ApJ 193, 585
Sivagnanam, P., Le Squeren, A.M., Foy, F., 1988, A&A 206, 285
Sivagnanam, P., Braz, M.A., Le Squeren, A.M., Tran Minh, F., 1990, A&A 233, 112
te Lintel Hekkert, P., 1990, Thesis, Leiden
te Lintel Hekkert, P., Zijlstra, A.A., 1991, Proc. ASA 9, 298
te Lintel Hekkert, P., Versteege-Hensel, H.A., Habing, H.J., Wiertz, M., 1989, A&AS 78, 399
te Lintel Hekkert, P., Caswell, J.L., Habing, H.J., Haynes, R.F., Norris, R.P., 1991, A&AS 90, 327
van der Veen, W.E.C.J., Rugers, M., 1989, A&A 226, 183
van Langevelde, H.J., van der Heiden, R., Schooneveld, C., 1990, A&A 239, 193
Wielen, R., 1977, A&A 60, 263
Wilson, W.J., Barrett, A.H., 1968, AJ 73, 209
Wood, P.R., Whiteoak, J.B., Hughes, M.G., Bessell, M.S., Gardner, F.F., Hyland, A.R., 1992, ApJ 397, 552

This article was processed by the author using Springer-Verlag TEX A&A macro package 1992.

© European Southern Observatory • Provided by the NASA Astrophysics Data System